An Ethylenamine Inhibitor Binds Tightly to Both Wild Type and Mutant HIV-1 Proteases. Structure and Energy Study

Tereza Skálová,* Jindřich Hašek, Jan Dohnálek, Hana Petroková, Eva Buchtelová, and Jarmila Dušková

Institute of Macromolecular Chemistry, Academy of Sciences of the Czech Republic, Heyrovského nám. 2, 162 06 Praha 6, Czech Republic

Milan Souček, Pavel Majer, Táňa Uhlíková, and Jan Konvalinka

Institute of Organic Chemistry and Biochemistry, Academy of Sciences of the Czech Republic, Flemingovo nám.2, 166 10 Praha 6, Czech Republic

Received October 24, 2002

An X-ray structure (resolution 2.2 Å) of mutant HIV-1 protease (A71V, V82T, I84V) complexed with a newly developed peptidomimetic inhibitor with an ethylenamine isostere Boc-Phe-Ψ-[CH_2CH_2NH]-Phe-Glu-Phe-NH_2, denoted as OE, is described and compared with the complex of wild-type HIV-1 protease with the same inhibitor (resolution 2.5 Å). OE shows tight binding to the wild type (K_i = 1.5 nM) as well as mutant (K_i = 4.1 nM) protease. The hydrogen bonds formed, in the case of hydroxyethylamine inhibitors, by a hydroxyl group are, in the case of OE inhibitors, replaced by a bifurcated hydrogen bond from the isosteric NH group to both catalytic aspartates Asp 25 and Asp 125. The binding modes of OE inhibitor to the wild type and mutant protease are similar. However, in the mutant protease, weaker van der Waals interactions of the mutated residues Val 84 and Val 184 with OE were found. This lack of interaction energy is compensated by a new aromatic hydrogen bond between the phenyl ring of the inhibitor in position P1 and the mutated residue Thr 182. Energy analysis based on molecular mechanics has been performed to distinguish between the static and dynamic backgrounds of disorder observed at the mutation sites Thr 82, Val 84, Thr 182, and Val 184.

Introduction

HIV-1 protease is a small aspartic protease with a monomer composed of 99 amino acid residues. It is active as a homodimer with monomers approximately symmetrically related by 2-fold axis. Residues Asp 25 and Asp 125 form a pair of catalytic aspartic acids, situated in the center of the binding site which is hidden under flaps. This protease belongs to the most studied proteins because of its important function during HIV (human immunodeficiency virus) life cycle.[1−3] It cleaves polyproteins of immature virus into functional proteins. The inhibition of the protease renders the virus noninfectious. Six inhibitors of the protease (Amprenavir, Indinavir, Lopinavir, Nelfinavir, Ritonavir, and Saquinavir[4]) are used in clinical practice as drugs against AIDS. However, during the course of treatment mutated forms of HIV protease are selected that are resistant toward one or more of protease inhibitors.

To analyze the interactions of HIV-1 protease with inhibitors, we have determined a structure of a mutant HIV-1 protease (A71V, V82T, I84V) complexed with peptidomimetic inhibitor Boc-Phe-Ψ[CH_2CH_2NH]-Phe-Glu-Phe-NH_2 (Figure 1). This inhibitor is denoted as OE, in correspondence with similar inhibitors of this series.[5−8] A special feature of this ethylenamine inhibitor is that it lacks an isosteric hydroxyl group, originally believed to be crucial for the tight binding of an inhibitor to an aspartic protease.[9] Despite this, OE has low inhibition constants both for the wild type and mutant protease (OE: K_i = 1.5 nM for wild-type, K_i = 4.1 nM for mutant).

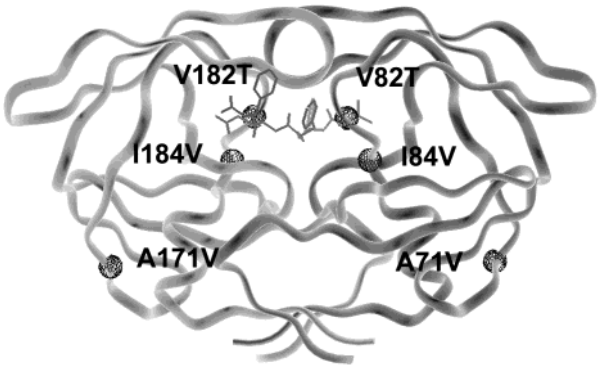

Figure 1. HIV-1 protease mutant (A71V, V82T, I84V) with the inhibitor OE bound in the active site. Positions of mutated residues in both chains are denoted.

The studied mutant protease contains three mutated residues which cause resistance to Indinavir (Indinavir: K_i = 0.52 nM for wild-type,[10] K_i = 12.7 nM for mutant[11]). Mutation A71V, being far from the active site, cannot directly influence the inhibitor binding. A71V was shown to be a compensatory mutation, improving catalytic efficiency of the protease having the primary mutations in positions 82, 84, or 90.[9] Changes in catalytic efficiency and inhibition constant were systematically studied by Schock et al.[12] (primary mutations V82T, I84V and compensatory mutations M46I, L63P). Mutations V82T and I84V affect directly

* Corresponding author. Tel: ++420 296809205. Fax: ++420 296809410. E-mail: skalova@imc.cas.cz.

10.1021/jm021079g CCC: $25.00
Published on Web 03/29/2003

the binding site. Mutation I84V is a frequent one and appears under the selection pressure of Amprenavir, Indinavir, Nelfinavir, Ritonavir, and Saquinavir.[13] Mutation V82T develops under selection pressure of Indinavir and Ritonavir.[13]

In the second part of the paper the OE binding to the mutant and wild-type HIV-1 protease is compared.

Several structural analyses describing changes in inhibitor binding to mutant HIV proteases have already been published. In some cases, mutations in the active site cause large geometrical change in inhibitor binding. This is the case of a structure deposited in the Protein Data Bank[14] under code 1hsg[15] (WT PR with Indinavir) in comparison with 1c6y[16] (L10V, K20M, L24I, S37D, M46I, I54V, L63P, A71V, V82T with Indinavir) or the case of 1hih[17] (WT PR with CGP53820, $K_i = 9$ nM) in comparison with 1hii[17] (HIV-2 protease with CGP53820, $K_i = 53$ nM).

In other cases, binding mode differences are small, sometimes despite large changes of inhibition constants. It was described in the case of 2bpx[18] (WT PR with Indinavir, $K_i = 0.38$ nM) in comparison with a nondeposited structure[19] (M46I, L63P, V82T, I84V with Indinavir, $K_i = 26$ nM), in the case of 1hvi[20] (WT PR with A77003, $K_i = 12$ nM) in comparison with 1hvs[21] (V82A with A77003, $K_i = 50$ nM) or in the case of 1odw[22] (WT PR with BMS182193, $K_i = 100$ nM) in comparison with 1odx[22] (A71T, V82A with BMS182193, $K_i = 800$ nM).

It seems that the relation between the inhibition constant and the inhibitor binding mode is not simple. It is difficult to interpret importance of small structural changes without detailed analysis of entropic and enthalpic changes. As an attempt to partly solve the problem, this paper includes an analysis of interaction energies and their comparison for the wild type and mutant protease−inhibitor complexes.

Results

HIV-1 PR Mutant−OE Complex. Structure Description. The structure refined to *R*-factor 20.3% and R_{free}-factor 25.2% consists of one dimer of the HIV-1 protease mutant (A71V, V82T, I84V) with the inhibitor OE bound in the active site in two alternative orientations, with 86 solvent water molecules and one molecule of β-mercaptoethanol. Average atom temperature factor is 35.0 Å^2. Data and structure characteristics are summarized in Table 1. The structure has been submitted to the Protein Data Bank under the access code 1lzq.

HIV-1 Protease. The density was interpretable with the exception of the flexible loop 35−43 at the ends of the flaps. Probably several alternative conformations exist in this region. Cis conformation of peptide bond Ser 137-Leu 138 was tested during a part of the refinement, because of positive peaks in $F_o - F_c$ map near Ser 137 O. Finally, the trans conformation was chosen as a more likely.

All side chains were localized in difference maps, and the correct conformation of side chains was checked by omit maps in ambiguous cases. The total occupancy of all non-hydrogen atoms is therefore held as full, with the exception of the C-terminal carboxyl groups. Deviations from the C_2 pseudo symmetry of the dimer occur namely in residues Met 36, Arg 41, Gln 61, and Asn 98, having different rotamers in chains A and B.

Radiation Damage. During the first part of refinement, strong spherical $F_o - F_c$ negative peaks above level 5σ appeared on one of the C-terminal oxygen atoms. Then the occupancy of the C-terminal CO_2^- group was refined to 0.58 in chain A and 0.56 in chain B. Results indicate that the crystal was partially damaged by strong radiation during measurement at the synchrotron source and that the C-terminal carboxyl groups are partly missing. Radicals probably appeared at the ends of both chains, and the terminal CO_2^- groups were gradually released by decarboxylation.[23,24] However, no marks of decarboxylation were observed on HIV-1 protease side chains in this structure.

Alternative Conformations. The protease contains alternative conformations of side chains in residues Ile 3, Glu 35, Phe 53, Ile 64, Cys 67, Thr 82, and Val 84 in chain A and the same residues in chain B (residues Ile 103, Glu 135, Phe 153, Ile 164, Cys 167, Thr 182, and Val 184). Both alternative conformations of Cys 67 (Cys 167, respectively) have two water molecules W352 and W357 (W351 and W369) in their vicinity. In residues Ile 50, Gly 51, Ile 150, and Gly 151 there are alternative conformations in main chain atoms because of a hydrogen bond that connects the flaps of both monomers. There are two possibilities: the flaps can be connected by a hydrogen bond between Ile 50 O and Gly 151 N (the first alternative conformation) or by a hydrogen bond between Ile 150 O and Gly 51 N (the second alternative conformation).

Water Molecules. Two water molecules are hidden in the active site: W370 is placed in the standard position between the inhibitor and the flaps; W331 has two alternative positions (I or Y) which are occupied according to the orientation of the bound inhibitor (I or Y), thus forming one hydrogen bond in each case (to Asp 129 or to Asp 29). Another 84 water molecules were localized in the first or in the second solvation shell (e.g., water W389 bound to the sulfur atom of BME).

β-Mercaptoethanol. In the PDB and PDBSum[25] there are two structures of HIV-1 protease that contain a bound molecule of BME: 1hih and 1dif. In both cases BME forms a disulfide bond either to Cys 67 or Cys 167. In our structure, the sulfur atom of BME is bound via hydrogen bond to Asp 129 O and the oxygen of BME forms a hydrogen bond to Trp 6 O. In the C_2 symmetry related position the density of the difference map was not so unambiguous, and water molecules were placed here (W344, W328, and W371).

Inhibitor. OE binding to the mutant HIV-1 protease is shown in Figure 2. The inhibitor was found in the active site of the dimer in two opposite (C_2 pseudo symmetric) alternative orientations (Figure 3). These two orientations of OE are denoted as conformations I and Y in the PDB file. The occupancy of the inhibitor in both orientations is 0.5. The $2F_o - F_c$ map was well defined with the exception of aromatic rings in positions P1 and P1′ where the peak of $2F_o - F_c$ density was present only between both alternative rings. A simulated annealing omit map indicates perpendicular orientations of the two rings, but the refinement keeps more parallel orientations.

The inhibitor is bound to the protease by 15 N−H···O or O−H···O hydrogen bridges with lengths in the range of 2.3−3.5 Å (Figure 4). The ester oxygen of

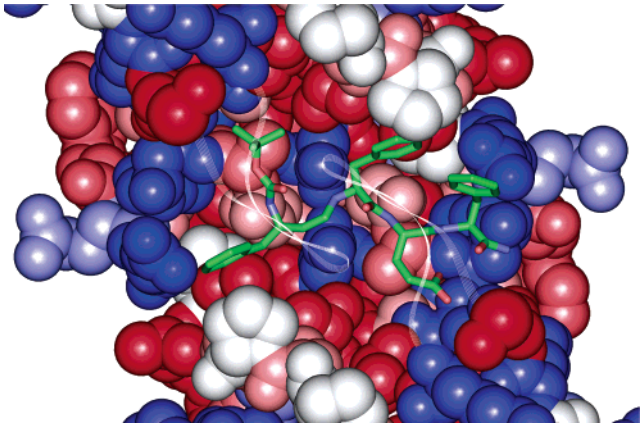

Figure 2. The view into the binding site of HIV-1 protease mutant (A71V, V82T, I84V) complexed with the inhibitor OE. Atoms at the bottom of the binding tunnel are displayed as van der Waals spheres and colored by the InsightII hydrophobicity spectrum. To enable a direct view into the active site, the flaps covering the binding tunnel above the inhibitor are displayed as thin transparent ribbons. The inhibitor OE is shown as a stick model.

BOC is connected by hydrogen bond to the buried water molecule W331 (which has an alternative position according to the inhibitor orientation). The second buried water molecule W370 mediates a connection from carbonyl groups of BOC and Phe in P1′ to the flaps. The nitrogen atom in the peptide bond isostere forms a bifurcated hydrogen bond to both catalytic residues Asp 25 and Asp 125. The inhibitor main chain nitrogen atoms in P1 and P2′, respectively, form hydrogen bonds to the carbonyls of Gly 127 and Gly 27. The glutamic acid in the S2′ binding pocket is bound via a network of six hydrogen bonds to Asp 29, Asp 30, and the water molecule W342. The nitrogen atom of P3′ Phe binds to the carbonyl of Gly 48 and has also a short intermolecular contact to Glu $O_{\epsilon 2}$ of P2′. The carbonyl of P3′ Phe binds to the nitrogen of Gly 48.

The alternative orientations of the inhibitor were refined without noncrystallographic symmetry. The maximum difference of interatomic distances corresponding to interactions between the inhibitor and the protease in both orientations was 0.3 Å. The inhibitor OE has slightly better electron density contours in orientation Y, and that is why the coordinates for energy analysis were taken from this orientation of the inhibitor.

Conformational Analysis. Mutated residues Thr 82, Val 84, Thr 182, and Val 184 with direct contacts to the disordered inhibitor were all found in alternative conformations. It can be expected that the 2-fold pseudo symmetry of the protease is partly violated by binding of an asymmetric inhibitor. Thus, it is possible that the alternative conformations of protease residues near the inhibitor binding site could be only "virtual", with one definite conformation of a residue interacting specifically with inhibitor in one definite orientation.

To resolve this question, an energy analysis of all possible combinations of conformations (residues 82, 84, 182, 184, and fixed orientation Y of the inhibitor) was

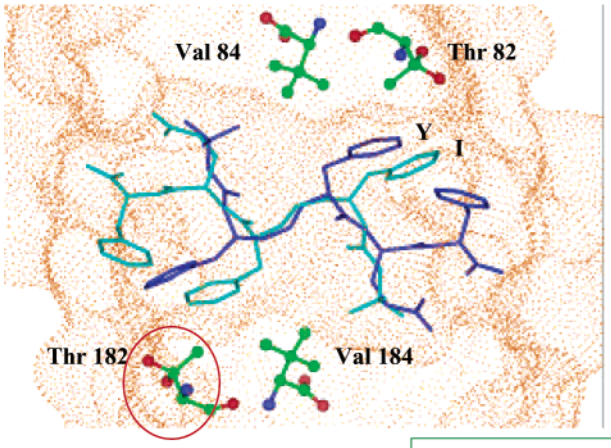

82 \ 182	T	-G	G
184 T			
84			
-G	8.86	8.10	8.13
G	8.61	8.10	4.49
T	8.30	7.60	9.84
184 T			
84			
-G	9.36	8.55	10.67
G	10.23	9.42	5.47
T	7.70	7.14	9.56
184 T			
84			
-G	9.88	9.04	11.25
G	9.70	8.21	4.98
T	7.77	6.51	9.03

82 \ 182	T	-G	G
184 T			
84			
-G	1.54	2.56	1.80
G	2.23	1.77	2.34
T	0.26	0.28	0.00
184 T			
84			
-G	2.88	0.88	0.91
G	1.69	1.69	1.70
T	0.61	0.41	0.51
184 T			
84			
-G	1.47	1.39	1.41
G	1.02	0.98	1.06
T	0.59	0.74	0.70

82 \ 182	T	-G	G
184 T			
84			
-G	6.05	5.61	6.90
G	6.27	5.93	6.97
T	5.02	4.14	5.90
184 T			
84			
-G	6.88	6.30	7.69
G	7.65	7.24	8.33
T	5.54	5.30	6.97
184 T			
84			
-G	6.08	5.62	6.86
G	5.99	5.89	6.51
T	5.31	2.99	5.07

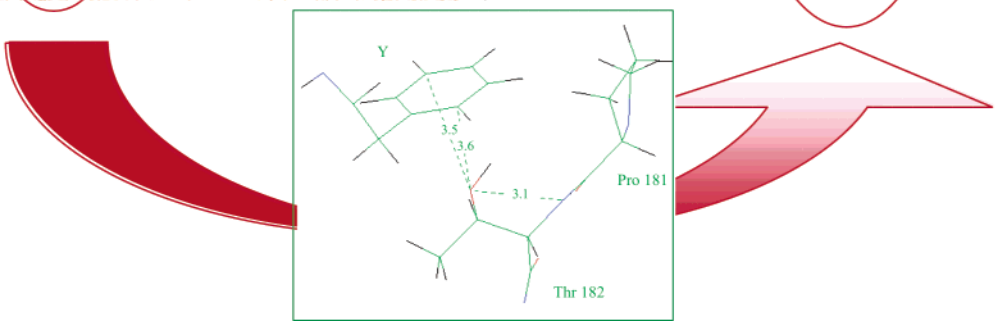

Figure 3. The conformational analysis of mutated residues in the active site of the HIV-1 protease mutant (A71V, V82T, I84V) complexed with the inhibitor OE. A view into the binding site from the side of the flaps shows the inhibitor (in orientations I and Y) and the mutated residues Thr 82, Val 84, Thr 182, and Val 184 (in alternative conformations). The table contains results of the conformational analysis comparing total interaction energies for all possible combinations of conformations of the residues 82, 84, 182, 184 and the inhibitor in orientation Y. The interaction energies are given in kcal/mol and are related to the strongest interaction (0 kcal/mol). The symbols G, −G, or T denote a category of the torsion angle χ_1 found in minimization, i.e., trans ~180°, −gauche ~ −60° or gauche ~ 60°. The aromatic hydrogen bond displayed on the scheme (corresponds also to Model 1 in Figure 8) appears in the states with lower energies (the middle column of the table).

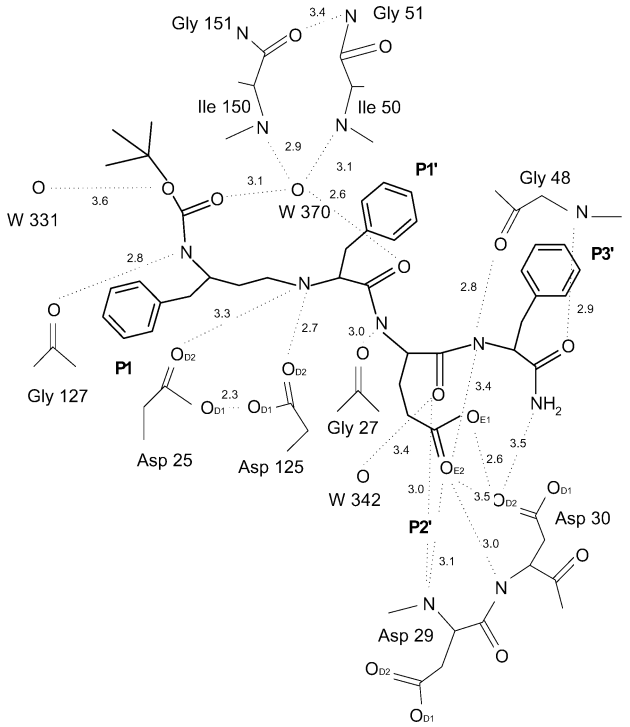

Figure 4. The network of hydrogen bonds formed between the HIV-1 protease mutant (A71V, V82T, I84V) and the inhibitor OE. All contacts that correspond to standard N−H···O and O−H···O hydrogen bonds up to 3.6 Å are denoted. The hydrogen bond connecting the protease flaps above the inhibitor (Gly 51 N−Ile 150 O) is added to the scheme.

performed using molecular mechanics. The structure with the inhibitor was minimized in all possible 81 combinations of conformations of residues 82, 84, 182, and 184. Then the total interaction energy was evaluated as a sum of interaction energies between the protease, inhibitor, and two water molecules in the active site. The total interaction energies that correspond to individual conformations are listed in Figure 3. These data show, that conformations of residues Val 84 and Val 184 have no important influence on the value of interaction energy. The interaction energy depends mainly on the conformation of residue Thr 182. The strongest interaction is connected with the minus gauche state of χ_1 torsion angle in residue Thr 182. This state corresponds to an aromatic hydrogen bond[26] between the aromatic ring in position P1′ and $O_{\gamma 1}$ of Thr 182. The fixed orientation of inhibitor Y probably entails a fixed conformation of Thr 182 with the aromatic hydrogen bond to the inhibitor. On the contrary, there are "real" alternative conformations in positions Thr 82, Val 84, Val 184 caused by rotational movement or different static conformations in individual protease molecules in the crystal.

Comparison of the Wild-type and Mutant Protease Complexes with OE. The structure of the wild-type HIV-1 protease complexed with the inhibitor OE has been solved by Petroková.[7] The superposition of the wild type and mutant proteases gave the root-mean-square deviation of positions of C_α atoms 0.35 Å. The Figure 5 shows that the inhibitor OE binds to the active site of the wild type and the (A71V, V82T, I84V) mutant

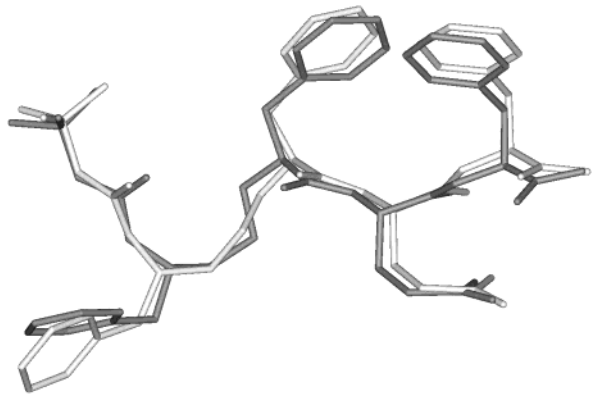

Figure 5. The comparison of conformations of the inhibitor OE in which it is bound to the wild-type HIV-1 protease (dark gray) and to the HIV-1 protease mutant (A71V, V82T, I84V). C_α atoms of the protease are superimposed.

proteases generally in a similar way. However, the closer inspection shows two significant differences in geometry.

First, there are differences in conformation of the peptide bond isostere. Torsion angles $C_\alpha-CH_2-CH_2-NH$ differ by −63° (wild type: −59° × mutant: −122°) and torsion angles $CH_2-NH-C_\alpha-C$ by 75° (wild type: −52° × mutant: 23°). As a result of this, the isosteric NH group that binds to Asp 25 and Asp 125 in the mutant complex is shifted further from the pseudo symmetry axis of the dimer and binds only to one aspartic acid of the catalytic pair in the wild-type structure, forming a new intramolecular hydrogen bond to BOC carbonyl oxygen.

Second, there are differences in the orientation of the phenyl ring Y302. However, due to the overlap of inhibitor bound in two orientations, the position of the phenyl ring in the mutant structure is not definitely determined from X-ray data, and an energy study is needed to determine interactions in this region.

Residue−residue interaction energy was studied for residues in a sphere within 10 Å radius around each of the "residues" of the inhibitor. The obtained interaction energies were summed up in two ways:

(1) By "residues" of the inhibitor as it is presented in Figure 6. From this point of view the interaction energy between the protease and the inhibitor has similar distribution in the wild type and mutant complexes.

(2) By selected residues of the protease. Interaction energies between the mutated residues (82, 84, 182, and 184) and the inhibitor show large differences (Figure 7):

Val/Thr 82. There is a similar interaction between the inhibitor and the native or mutated residue 82. The main contribution to the interaction energy is formed by van der Waals interaction between Phe Y303 and Val/Thr 82.

Ile/Val 84 and Ile/Val 184. The interaction has also mainly a van der Waals character and is approximately by 1.3 kcal/mol stronger for the wild-type protease (Ile at positions 84, 184).

Val/Thr 182. The interaction has a van der Waals as well as Coulombic basis and is approximately by 1.5 kcal/mol stronger in the case of the mutant (Thr 182).

Deformation energy of the OE inhibitor (conformational energy difference between its free and bound

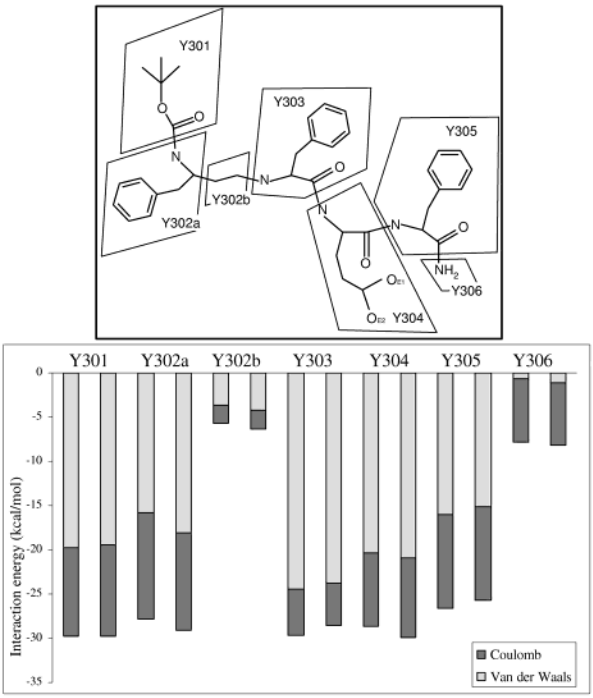

Figure 6. Van der Waals and Coulomb interaction energies between "residues" of the inhibitor OE and its neighbors up to 10 Å. A comparison of the wild type (the first column for each residue) and the mutant complexes (the second column for each residue). The division of the inhibitor into the "residues" is explained in the scheme above. Inhibitor−inhibitor interactions for individual "residues" are included (together with the interactions to the two buried water molecules); therefore, it is not possible to calculate the interaction energy of the inhibitor as a sum of interaction energies of all "residues". Values are in kcal/mol.

state) is similar in the cases of the wild type and mutant proteases: conformational energies of OE bound to both HIV-1 proteases differ approximately by 0.2 kcal/mol.

Discussion

Our energy studies showed a similar distribution of interaction energies across the "residues" of the inhibitor in the mutant and wild type protease, and it is in correspondence with similar inhibition constants of OE for both types of HIV-1 protease. The differences were found in the interactions between OE and residues Val/Thr 82, Ile/Val 84, Val/Thr 182, and Ile/Val 184. One of rotamers of residues 84 and 184 in the mutant complex remains exactly in the same position as in the wild type complex, only $C_{\delta 1}$ atom of isoleucine is "missing" in the case of valine. The unfilled cavity between OE and these mutated residues causes weaker van der Waals interactions between OE and HIV-1 protease in the mutant case in a similar way as in previously published mutational analyses.[19] This decrease in interaction energy between OE and mutant HIV-1 protease is compensated by forming the aromatic hydrogen bond between Thr 182 and Phe Y302. This favorable interaction may be the reason the inhibitor OE tightly binds also to the mutant protease, unlike inhibitors in other structural studies where the mutation on the residue 82 caused unfavorable interactions.[19,21,22]

Mutated Residue Thr 182. For a better understanding of the mutated residue Thr 182 interactions, a comparison of X-ray and computational structures is shown in Figure 8. In the X-ray structure, the phenyl rings of the Y302 and I204 residues of the opposite orientations of OE are placed near to each other. A broad maximum of the $2F_o - F_c$ map placed between both rings makes it difficult to interpret the interactions in detail. Model 1 (the "global" minimum found by conformational analysis) and Model 2 (the minimized final X-ray structure which was used in the interaction energy comparison) are also approximately in agreement with $2F_o - F_c$ and $F_o - F_c$ maps.

Both models and the X-ray structure show similar hydrogen bond patterns around Thr 182 hydroxyl: the aromatic hydrogen bond to the phenyl ring of Y302 group in the inhibitor, the hydrogen bond to the main chain NH group of Thr 182 and O−H···O type bond to the main chain carbonyl group of Pro 181. These bonds change as follows:

Model 1. The oxygen atom of Thr 182 hydroxyl lies approximately above the center of the phenyl ring of the Y302 group of the inhibitor. The perpendicular distance between the oxygen atom and the phenyl ring is 3.2 Å, and all distances from Thr 182 O to the carbon atoms of the phenyl group are in the range of 3.5−3.6 Å. The N−H···O (Thr 182) distance is 3.1 Å and the O−H···O (Pro 181) hydrogen bond distance is 3.2 Å.

Model 2. The aromatic hydrogen bond to Phe Y302 (distance from $O_{\gamma 1}$ Thr 182 to $C_{\delta 1}$ Phe Y302 is 3.3 Å and to $C_{\epsilon 1}$ Phe Y302 is 3.4 Å). The N−H···O (Thr 182) distance is 3.0 Å and the O−H···O (Pro 181) hydrogen bond distance is 3.1 Å.

X-ray Structure. The hydroxyl group of Thr 182 forms a close contact only to $C_{\epsilon 1}$ Phe Y302 with a distance of 3.4 Å. The N−H···O (Thr 182) distance is 2.9 Å and the O−H···O (Pro 181) hydrogen bond distance is 3.6 Å.

The result is that the conformation of Thr 182 is determined by competition of three hydrogen bonds, two of them to the main chain NH and CO groups with stable geometry and one to the Y302 phenyl which has conformational freedom in the S1 pocket.

Conclusion

As opposed to hydroxyethylene or hydroxyethylamine inhibitors the group of ethylenamine inhibitors has not been analyzed from the structural point of view until now. This paper gives an experimental evidence of the binding mode of the ethylenamine inhibitor OE (Boc-Phe-Ψ[CH_2CH_2NH]-Phe-Glu-Phe-NH_2) to the HIV-1 protease mutant (A71V, V82T, I84V). Binding of the isosteric hydroxyl group to catalytic aspartates Asp 25 and Asp 125 described as one of the main reason of excellent properties of hydroxyethylamine and hydroxyethylene inhibitors is in the case of ethylenamine inhibitors successfully replaced by hydrogen bonds from the NH group of the isoster. The CH_2CH_2NH group gives the inhibitor more flexibility in the center of the active site. It gives more freedom also to the side chains of the inhibitor and allows them to fit the binding pockets more easily.

The inhibitor OE is bound to the protease by an extensive network of hydrogen bonds. Hydrogen bond donors are often surrounded by several possible acceptors and even small changes of the positions of the inhibitor atoms cause weakening of some hydrogen bonds while making other stronger. This extensive

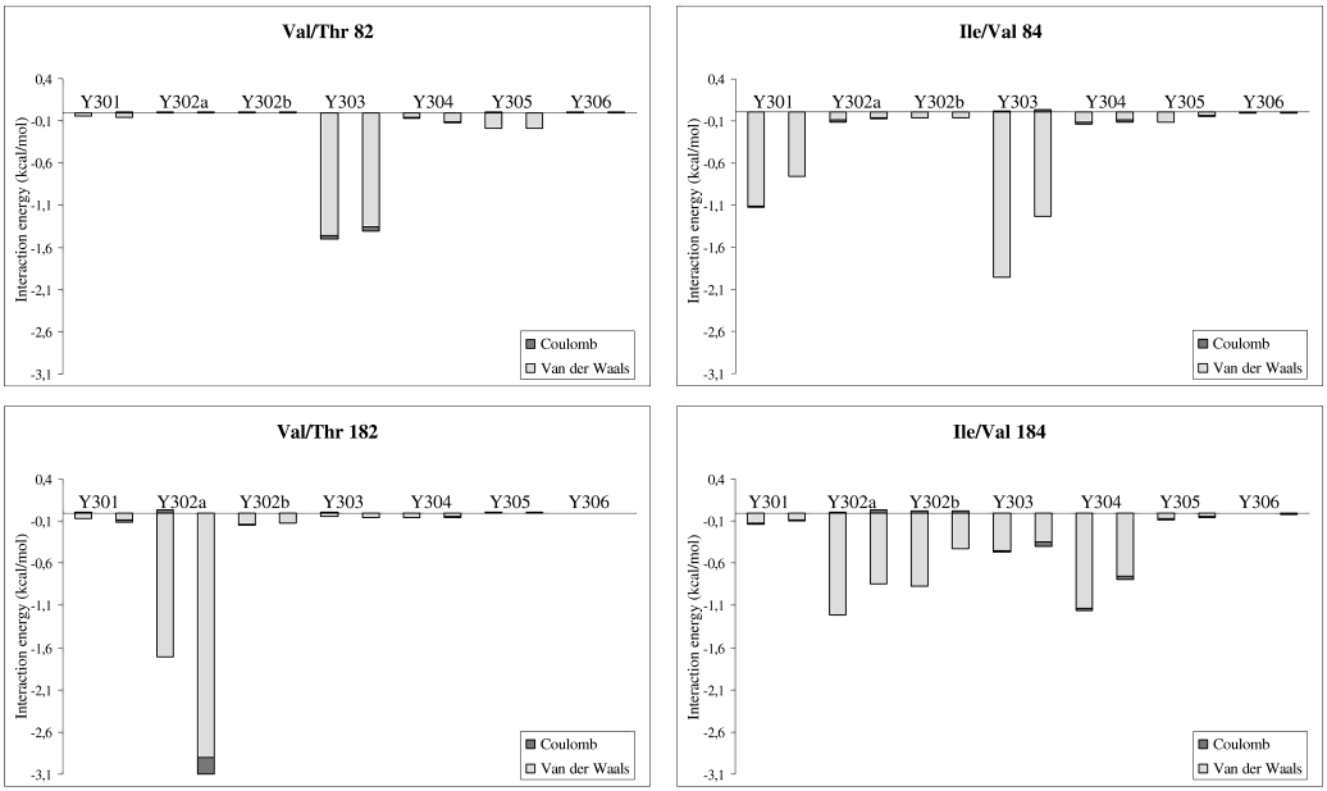

Figure 7. Interaction energies between the "residues" of the inhibitor OE and the individual mutated residues of HIV-1 protease, as extracted from total values denoted in the previous table. The first column for each residue shows the interaction in the wild-type complex, the second column in the mutant complex.

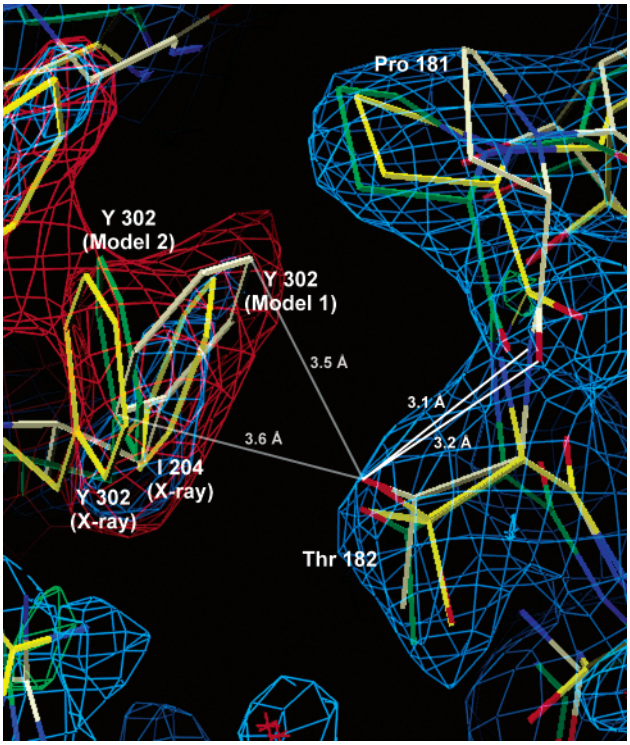

Figure 8. The mutated residue Thr 182 of the studied HIV-1 protease mutant (A71V, V82T, I84V) and its interaction with the phenyl ring of Y302 of the inhibitor OE. A $2F_o - F_c$ map at the level of 1σ (blue) and an $F_o - F_c$ simulated annealing omit map of the inhibitor at level 3σ (red) are shown. The X-ray structure (yellow) and two optimized structures, Model 1 (white; the "global" minimum from conformational analysis) and Model 2 (green; the minimized X-ray structure used for evaluation of interaction energies) are compared.

flexible network of hydrogen bonds thus allows higher conformational freedom of the inhibitor and gives the protease−inhibitor complex a wider variety of low energy states contributing to a better stability of the complex in terms of entropy.

A more detailed analysis was devoted to another effect observed in the mutant HIV-1 PR complexed with the OE inhibitor—all four mutated side chains oriented to the inhibitor binding tunnel were found in alternative conformations. Conformational analysis proved that the energetically most favorable state forms an aromatic hydrogen bond between OE and the mutated residue Thr 182 and that the alternative conformations of other three disordered mutated residues are approximately energetically equivalent.

It was also shown that the mutation of HIV-1 protease influences the inhibition properties by mainly two factors. In the mutant complex of HIV-1 PR with OE inhibitor the energy gain received from an additional aromatic hydrogen bond between Thr 182 and the phenyl ring of the inhibitor OE in position P1 compensates for stronger van der Waals interactions between the inhibitor and Ile 84, Ile 184 in the wild-type complex, and therefore the total interaction energy between OE and HIV-1 protease remains similar in both cases. It is in agreement with similar inhibition constants for the wild type and mutant proteases.

Experimental Section

Peptide Synthesis. Tripeptide TFA·H-Phe-Glu-Phe-NH_2 was synthesized by conventional solution-phase methodology using Boc/Bzl chemistry. Purity of the peptide was checked by analytical HPLC on a Vydac C_{18} column and amino acid analysis.

Synthesis of Boc-Phe-ψ[CH_2CH_2NH]-Phe-Glu-Phe-NH_2. A solution of $NaBH_3CN$ (153 mg, 2.4 mM) in MeOH (5 mL) was added dropwise to a stirred solution of TFA·H−Phe-Glu-Phe-NH_2 (553 mg, 1.0 mM) and freshly prepared Boc-NHCH($CH_2C_6H_5$)CH_2CHO[28] (248 mg, 1.0 mM) in 1% AcOH/MeOH (10 mL) at room temperature. After 16 h the solvent was removed in vacuo, and the residue was extracted with ethyl acetate (3 × 10 mL). Combined extracts were washed successively with aqueous 1 M $NaHCO_3$, 1 M $KHSO_4$, and brine. The organic layer was dried over $MgSO_4$, and the solvent was removed under reduced pressure. The residue was triturated with diethyl ether and dried in a desiccator over P_2O_5 to give the product in 63% yield, mp 208−215 °C.

High-resolution mass spectrum was measured on a ZAB-EQ (VG Analytical) using the FAB technique (Xe, 8 kV): HRMS (FAB) $C_{38}H_{49}N_5O_7$ required 687.36317; found 688.3686 $[M + 1]^+$.

Expression and Purification of Recombinant Proteases. The DNA coding region for engineered HIV-1 PR (A71V, V82T, I84V) was amplified from corresponding site-mutated proviral clones[29] using internal pair of PCR primers HIV 1_{in} (5′-TAGAATTCATATGAGAGACAACAACTCCCCCT-3′) including *Eco RI* and *Nde I* sites at the 5′ end, and HIV 2_{in} (5′-GGGGATCCTTACTATGGTACAGTCTCAATAGG-3′) including a *Bam HI* restriction site at its 5′-terminus. The PR coding region and the adjacent sequences encoding for the first 21 amino acids of the *pol* polyprotein were cloned into the pET24a expression vector (Novagen).

The host strain *Escherichia coli* BL21 (DE3) (Novagen) was used to overexpress the PR precursors. The construction and expression of HIV PR variants were performed using pET24a expression vector. Proteases were purified from inclusion bodies by solubilization in urea followed by chromatography on QAE-Sephadex and FPLC on Mono S-Sepharose (Pharmacia) as described previously.[30]

Activity and Inhibition Assay. Inhibition constants were determined by a spectrophotometric assay with the chromogenic peptide substrate KARVNle*NphEANle-NH_2, as described previously.[30] Typically, 8 pM of a protease preparation was added to 1 mL 0.1 M sodium acetate buffer, pH 4.7, 0.3 M NaCl and 4 mM EDTA, containing 20 nmol of substrate and various concentrations of the inhibitor dissolved in DMSO. The final concentrations of DMSO were kept below 2.5%. The substrate hydrolysis was followed as a decrease of absorbance at 305 nm using an Aminco Bowman DW2000 spectrophotometer. Both K_i values are the averages of three determinations.

Crystallization. The solution of HIV-1 protease (in 50 mM Na acetate buffer pH 5.8 with 1 mM EDTA and 0.05% BME) concentrated to 3 mg/mL was inhibited by 4-fold molar excess of inhibitor dissolved in DMSO. Crystals with dimensions 0.05 × 0.05 × 0.2 mm of hexagonal rod appearance were obtained by microseeding and using mother liquor of 0.5 M NaCl in 0.1 M Na-acetate buffer, pH 4.4, and 10−15% of glycerol. The seed solution was prepared by crushing a small needlelike crystal in a little amount of mother liquor without glycerol and diluting 10^2−10^6 times with the same solution. Glycerol in crystallization solution was found to improve the crystal size and properties. Before freezing, crystals were soaked in mother liquor with 20% glycerol for 30 s.

Data Collection and Processing. X-ray diffraction of the crystal was measured at the source of synchrotron radiation ESRF in Grenoble using a microdiffractometer[31] (with high flux on the sample) on the beam line ID14-1 at 100 K using wavelength $\lambda = 0.934$ Å and exposure time 30 s per frame. The quality of the diffraction decreased during the measurement. Data were measured using oscillation method in three series, with three different positions on the needle-shaped crystal. Only the first part of each series was suitable for processing; the reflections measured later (after 10−20 min of measurement) were split.[32] The suitable data were processed and scaled using programs Denzo and Scalepack from the HKL package[33] and the software package CCP4.[34] The results are summarized in Table 1.

Table 1. Data and Structure Characteristics of the HIV-1 Protease Mutant (A71V, V82T, I84V) Complexed with the Inhibitor OE

resolution range [Å]	33.0−2.2
space group	$P6_1$
unit cell: *a*, *b*, *c* [Å]	62.68, 62.68, 83.31
α, β, γ [deg]	90, 90, 120
number of reflections	61979
number of unique reflections	9490
mosaicity [deg]	0.19
data completeness [%]	99.9
R_{merge} [%]	7.9
overall *B*-factor from Wilson plot [Å^2]	31.8
R [%]	20.3
R_{free} [%] (test set: 5.9% of data)	25.2
RMSD from ideal bond lengths [Å]	0.01
RMSD from ideal valence angle values [deg]	1.6
average atom temperature *B*-factor [Å^2]	35.0
number of water molecules	86

Structure Determination. The structure was refined using the CNS software package.[35] A symmetrized structure of HIV-1 protease taken from a structure with a similar inhibitor[8] was used as a model for rigid body refinement. After rigid body refinement and simulated annealing the protease was refined with pseudo C_2 noncrystallographic symmetry restraints of the dimer. The symmetry restraints were partly released in later stages of the refinement. They were held on 75 of 99 residues at the end of the refinement with a force constant 200 kcal/(mol·Å^2). Alternative conformations of residues were refined with zero distance restraints between positions of common atoms. The inhibitor was first placed into the difference $F_o - F_c$ map in one orientation. Then the inhibitor in an opposite orientation was positioned into remaining positive peaks of the $F_o - F_c$ map in the binding site. The solvent molecules (86 water molecules and 1 BME) were localized gradually in later stages of the refinement checking R_{free} and correct geometry. The basic structure characteristics are listed in the second part of Table 1.

The structure was refined with constraints to standard geometry described in the CNS standard parameter files protein_rep.param and water_rep.param.[35] A parameter file was prepared for the inhibitor and β-mercaptoethanol molecules to fit geometry of molecular fragments found in the Cambridge Structural Database.[36] The refinement was done using the maximum likelihood method. The last run of refinement (all reflections included) was performed using the residual method. The final refinement characteristics are summarized in Table 1. The higher *B* values may correspond to a slow degradation of the crystal during measurement.

The Ramachandran plot[27] shows standard distribution of φ, ψ torsion angle values in the protein (93.1% in most favored regions and 6.9% in additional allowed regions). Reliability of the structure was tested by program Procheck[27] with good results. Error in coordinates estimated from Luzzati plot is 0.3 Å.

The figures were made with programs InsightII,[37] ISISDraw 2.3,[38] WebLabViewerPro,[39] and program O.[40]

Molecular Modeling. All energy evaluations for mutant and wild-type complexes were done by the program Discover in the software package InsightII.[37] The starting geometry for molecular modeling was taken from the X-ray structure. Alternative conformations with lower occupancies and the inhibitor in orientation I were removed from the measured structures and hydrogen atoms were added by the Builder in InsightII. Ionization of amino acids corresponds to pH 5. The hydrogen atoms in the neighborhood of the inhibitor OE in orientation Y were added in agreement with the network of hydrogen bonds found by X-ray diffraction.

Structures were optimized in the force field cff91. Only water molecules determined by X-ray structure analysis were included in the optimization. All oxygen atoms of crystallographic water molecules were fixed in their experimentally found positions during minimization. Only two water molecules buried inside the binding site (W 370 placed between

the flaps and the inhibitor and W 331 in its alternative position Y) were minimized without constraints. The computations were performed with dielectric constant $\epsilon = 4$ which yields the best agreement between measured and modeled lengths of hydrogen bonds. Nonbonded interactions were cut off at distance 15 Å. Energy minimization was done in several steps using steepest descent and then conjugate gradient methods. Only hydrogen atoms were relaxed at the first stage of minimization. Then the protein backbone was fixed, and heavy atoms were tethered for a part of this step to find an energetic minimum with a conformation very similar to the X-ray structure. In the final stages of minimization all atoms were released. The structures were minimized until maximum derivatives were less than 0.01 kcal/Å.

For the interaction energy comparisons between the mutant and wild-type complexes water molecules were removed with the exception of two buried water molecules. Then the system was minimized again.

The network of hydrogen bonds found in the X-ray structure was reliably reproduced in the energy-minimized structure. The binding pocket surrounding the asymmetric inhibitor follows its asymmetry closer in the structure after energy minimization than in the experimental structure.

RMSD on C_α positions between the measured and minimized structures in the whole protein is 0.7 Å. The largest differences between the experimental and minimized structures are in the flap regions. There the C_α positions differ by up to 1.7 Å. These differences seem to be caused by conformational flexibility of the flaps which is higher for a free complex without crystal contacts. Most differences in positions of non-hydrogen atoms of the inhibitor (up to 1.7 Å) are in the phenyl rings in P1 and P1′ positions of which was not exactly determined by X-ray structure analysis. In the rest of the inhibitor these differences are lower than 0.8 Å.

Acknowledgment. The research was supported by the Grant Agency of the Academy of Sciences of the Czech Republic (projects A4050811/1998 and KJB4050312/2003), Grant Agency of the Czech Republic (projects no. 203/98/K023, 204/00/P091, and 203/00/D117), by the Academy of Sciences of the Czech Republic (projects AVOZ4050913 and Z4 055 905) and by the grant NI/6339-3 from the Ministry of Health Care of the Czech Republic. The authors thank to the ESRF in Grenoble for providing beamtime and Hassan Belrhali for help.

Appendix

Abbreviations: HIV-1, human immunodeficiency virus type 1; Boc, *tert*-butoxycarbonyl; OE, Boc-Phe-Ψ-[CH_2CH_2NH]-Phe-Glu-Phe-NH_2; AIDS, acquired immunodeficiency syndrome; WT, wild-type; PR, protease; BME, β-mercaptoethanol; PDB, The Protein Data Bank; HRMS, high-resolution mass spectrometry; TFA, trifluoroacetic acid; EDTA, ethylenediaminetetraacetic acid; DMSO, dimethyl sulfoxide; FAB, fast atom bombardment; Nph, 4-nitrophenylalanine; Nle, norleucin; RMSD, root-mean-square deviation.

References

(1) Babine, R. E.; Bender, S. L. Molecular recognition of protein−ligand complexes: Applications to drug design. *Chem. Rev.* **1997**, *97*, 1359−1472.
(2) Garg, R.; Gupta, S.; Gao, H.; Babu, M.; Debnath, A.; Hansch, C. Comparative quantitative structure−activity relationship on anti-HIV drugs. *Chem. Rev.* **1999**, *99*, 3525−3567.
(3) Leung, D.; Abbenante, G.; Fairlie, D. Protease inhibitors: current status and future prospects. *J. Med. Chem.* **2000**, *43*, 305−341.
(4) National Institute of Allergy and Infectious Diseases, National Institutes of Health, www.niaid.nih.gov/daids/.
(5) Dohnálek, J.; Hašek, J.; Dušková, J.; Petroková, H.; Hradílek, M.; Souček, M.; Konvalinka, J.; Brynda, J.; Sedláček, J.; Fábry, M. A distinct binding mode of a hydroxyethylamine isostere inhibitor of HIV-1 protease. *Acta Crystallogr. D* **2001**, *57*, 472−476.
(6) Dohnálek, J.; Hašek, J.; Dušková, J.; Petroková, H.; Hradílek, M.; Souček, M.; Konvalinka, J.; Brynda, J.; Sedláček, J.; Fábry, M. Hydroxyethylamine isostere of an HIV-1 protease inhibitor prefers its amine to the hydroxy group in binding to catalytic aspartates. A synchrotron study of HIV-1 protease in complex with a peptidomimetic inhibitor. *J. Med. Chem.* **2002**, *45*, 1432−1438.
(7) Petroková, H. Unpublished results. Complex of native HIV-1 protease with OE inhibitor crystallized in $P6_1$, $a = b = 61.2$ Å, $c = 82.3$ Å, measured to diffraction limit 2.5 Å, refined to $R = 18.0\%$, $R_{free} = 24.5\%$ will be available in PDB under the code 1m0b.
(8) Hašek, J.; Dohnálek, J.; Dušková, J.; Konvalinka, J.; Hradilek, M.; Souček, M.; Sedláček, J.; Brynda, J.; Buchtelová, E. Antiretroviral Drug Design Based on Structure Analysis of Proteases. *Mater. Struct.* **1998**, *5B*, 437−438.
(9) Wlodaver, A.; Vondrášek, J. Inhibitors of HIV-1 protease: A major success of structure-assisted drug design. *Annu. Rev. Bioph. Biomol. Struct.* **1998**, *27*, 249−284.
(10) Dorsey, B. D.; Levin, R. B.; McDaniel, S. L.; Vacca, J. P.; Guare, J. P.; Darke, P. L.; Zugay, J. A.; Emini, E. A.; Schleif, W. A.; Quintero, J. C.; Lin, J. H.; Chen, I. W.; Holloway, M. K.; Fitzgerald, M. D.; Axel, M. G.; Ostovic, D.; Anderson, P. S.; Huff, J. R. L-735,524: The design of a potent and orally bioavailable HIV protease inhibitor. *J. Med. Chem.* **1994**, *37*, 3443−3451.
(11) Weber, J. Inhibition of HIV-1 protease: kinetics, resistance, structure and function. Ph.D. Thesis, Institute of Organic Chemistry and Biochemistry, Academy of Sciences of the Czech Republic, Prague, 2000.
(12) Schock, H. B.; Garsky, V. M.; Kuo, L. C. Mutational anatomy of an HIV-1 protease variant conferring cross-resistance to protease inhibitors in clinical trials. *J. Biol. Chem.* **1996**, 31957−31963.
(13) HIVresistanceWeb, www.hivresistanceweb.com.
(14) The Protein Data Bank. *Nucleic Acids Res.* **2000**, *28*, 235−242; www.rcsb.org/pdb.
(15) Chen, Z.; Li, Y.; Chen, E.; Hall, D.; Darke, P.; Culberson, C.; Shafer, J.; Kuo, L. Crystal structure at 1.9 Å resolution of Human immunodeficiency virus (HIV) 2 protease complexed with L-735,524, an orally bioavailable inhibitor of the HIV proteases. *J. Biol. Chem.* **1994**, *269*, 26344−26348.
(16) Munschi, S.; Chen, Z.; Yan, Y.; Li, Y.; Olsen, D. B.; Schock, H. B.; Galvin, B. B.; Dorsey, B. and Kuo, L. C. An alternate binding site for P1−P3 group of a class of potent HIV-1 protease inhibitors as a result of concerted structural change in the 80s loop of the protease. *Acta Crystallogr. D* **2000**, *56*, 381−388.
(17) Priestle, J. P.; Fässler, A.; Rössel, J.; Tintelot-Blomley, M.; Strop, P. and Grüter, M. G. Comparative analysis of the X-ray structures of HIV-1 and HIV-2 proteases in complex with CGP 53820, a novel pseudosymmetric inhibitor. *Structure* **1995**, *3*, 381−389.
(18) Munschi, S.; Chen, Z.; Li, Y.; Olsen D. B.; Fraley, M. E.; Hungate, R. W.; Kuo, L. C. Rapid X-ray diffraction analysis of HIV-1 protease-inhibitor complexes: inhibitor exchange in single crystals of the bound enzyme. *Acta Crystallogr. D* **1998**, *54*, 1053−1060.
(19) Chen, Z.; Li, Y.; Schock, H. B.; Hall, D.; Chen, E.; Kuo, L. C. Three-dimensional Structure of a Mutant HIV-1 Protease Displaying Cross-resistance to All Protease Inhibitors in Clinical Trials. *J. Biol. Chem.* **1995**, *270*, 21433−21436.
(20) Hosur, M. V.; Bhat, T. N.; Kempf, D. J.; Baldwin, E. T.; Liu, B.; Gulnik, S.; Wideburg, N. E.; Norbeck, D. W.; Appelt, K.; Erickson, J. W. Influence of stereochemistry on activity and binding modes for C_2 symmetry-based diol inhibitors of HIV-1 protease. *J. Am. Chem. Soc.* **1994**, *116*, 847−855.
(21) Baldwin, E. T.; Bhat, T. N.; Liu, B.; Pattabiraman, N.; Erickson, J. W. Structural basis of drug resistance for the V82A mutant of HIV-1 proteinase. *Struct. Biol.* **1995**, *2*, 244−249.
(22) Kervinen, J.; Thanki, N.; Zdanov, A.; Tino, J.; Barrish, J.; Lin, P. F.; Colonno, R.; Riccardi, K.; Samanta, H.; Wlodawer, A. Structural analysis of the native and drug-resistant HIV-1 proteinases complexed with an aminodiol inhibitor. *Protein Pept. Lett.* **1996**, *3*, 399−406.
(23) Burmeister, W. P. Structural changes in a cryo-cooled protein crystal owing to radiation damage. *Acta Crystallogr. D* **2000**, *56*, 328−341.
(24) Ravelli, R. B. G.; McSweeney, S. M. The 'fingerprint' that X-rays leave on structures. *Structure* **2000**, *8*, 315−328.
(25) PDBSum, www.biochem.ucl.ac.uk/bsm/pdbsum.
(26) Desiraju, G. R.; Steiner, T. *The weak hydrogen bond*; Oxford University Press: New York, 1998.
(27) Laskowski, R. A.; MacArthur, M. W.; Moss, D. S.; Thornton, J. M. Procheck−a program to check the stereochemical quality of protein structures. *J. Appl. Crystallogr.* **1993**, *26*, 283−291.

(28) Souček, M.; Urban, J. An Efficient Method for Preparation of Optically active N-Protected α-Amino Aldehydes from N-Protected α-Amino Alkohols. *Collect. Czech. Chem. Commun.* **1995**, *60*, 693−696.
(29) Weber, J.; Mesters, J. R.; Lepšík, M.; Prejdová, J.; Švec, M.; Šponarová, J.; Mlčochová, P.; Stříšovský, K.; Uhlíková, T.; Souček, M.; Machala, L.; Staňková, M.; Vondrášek, J.; Klimkait, T.; Kraeusslich, H. G.; Hilgenfeld, R and Konvalinka, J. Unusual binding mode of an HIV-1 protease inhibitor explains its potency against multi-drug-resistant HIV strains. *J. Mol. Biol.* **2002**, *324*, 739−754.
(30) Konvalinka, J.; Litera, J.; Weber, J.; Vondrášek, J.; Hradílek, M.; Souček, M.; Pichová, I.; Majer, P.; Štrop, P.; Sedláček, J.; Heuser, A. M.; Kottler, H.; Kräusslich, H. G. Configurations of diastereomeric hydroxyethylene isosteres strongly affect biological activities of a series of specific inhibitors of human-immunodeficiency-virus protease. *Eur. J. Biochem.* **1997**, *250*, 559−566.
(31) Perrakis, A.; Cipriani, F.; Castagna, J. C.; Claustre, L.; Burghammer, M.; Riekel, C.; Cusack, S. Protein microcrystals and the design of a microdiffractometer: current experience and plans at EMBL and ESRF/ID13. *Acta Crystallogr. D* **1999**, *55*, 1765−1770.
(32) Skálová, T.; Hašek, J.; Dohnálek, J.; Petroková, H.; Buchtelová, E. Mutant HIV-1 protease complexed with tetrapeptide inhibitor. Preliminary report. *Acta Phys. Pol. A* **2002**, *101*, 659−663.
(33) Otwinowski, Z.; Minor, W. Processing of X-ray Diffraction Data Collected in Oscillation Mode. In *Methods in Enzymology, Volume 276: Macromolecular Crystallography, part A*; Carter, C. W., Jr., and Sweet, R. M., Eds.; Academic Press: New York, 1997; pp 307−326.
(34) Collaborative Computational Project, Number 4. The CCP4 Suite: Programs for Protein Crystallography. *Acta Crystallogr. D* **1994**, *50*, 760−763.
(35) Brunger, A. T.; Adams, P. D.; Clore, G. M.; Delano, W. L.; Gros, P.; Grosse-Kunstleve, R. W.; Jiang, J. S.; Kuszewski, J.; Nilges, N.; Pannu, N. S.; Read, R. J.; Rice, L. M.; Simonson, T.; Warren, G. L. Crystallography & NMR System: A New Software Suite for Macromolecular Structure Determination. *Acta Crystallogr. D* **1998**, *54*, 905−921.
(36) The Cambridge Structural Database, http://www.ccdc.cam.ac.uk.
(37) InsightII, Molecular Simulations Inc., 2000.
(38) ISISDraw 2.3, MDL Information Systems, 2000.
(39) WebLabViewerPro, Molecular Simulations Inc., 2000.
(40) Jones, T. A.; Kjeldgaard, M. *O−the manual version 5.9*; Department of Molecular Biology, BMC, Uppsala University, Sweden and Department of Chemistry, Aarhus University, Denmark, 1993.

JM021079G